Acoustic Emission Monitoring of Pre-Stressed Concrete Beams During Accelerated Corrosion of Pre-Stressing Tendons

SADEGH MAHMOUDKHANI, JUNHUI ZHAO,
JASMIN COCHINGCO, AFTAB MUFTI
and DOUGLAS THOMSON

ABSTRACT

Acoustic sensors attached to pre-stressed/post-tensioned bridges are promising tools for monitoring the progression of corrosion damage in pre-stressing/post-tensioning tendons. In this study, acoustic emission signals from a pre-stressed beam containing three pre-stressed tendons that were exposed to accelerated corrosion conditions were studied. A short length of each tendon was exposed, and a tank filled with the NaCl solution was placed over the exposed tendon. Over a period of several months, a corrosion current was driven into the tendons until at least one wire corroded through. Acoustic sensors were attached along the beam and were used to record acoustic emission events during the accelerated corrosion. At the termination of the accelerated corrosion experiment, the beam was sliced into sixty-two cross-sections, each being 5 cm thick. Each slice was inspected to correlate corrosion and tendon slippage with acoustic emission signals. Maps of the estimated origin of acoustic emission signals were compared with the maps of the position of tendon corrosion and slippage. The acoustic emission signals were correlated with the presence of wire fracture due to corrosion on the tendon and with proximity to the end of the beam. The larger emission signals are likely due to the loss of bond between the tendons and concrete, as tendon fracture due to corrosion was not found in any of the cross-sections. This work points to the use of acoustic emission to track the progression of damage in cases where corrosion has already resulted in tendon fracture, and progression is proceeding by loss of bond.

Sadegh Mahmoudkhani, Department of Civil Engineering, University of Manitoba, Winnipeg, Manitoba, R3T 2N2, Canada
Junhui Zhao, Department of Electrical and Computer Engineering, University of Manitoba, Winnipeg, Manitoba, R3T 2N2, Canada
Jasmin Cochingco, Department of Electrical and Computer Engineering, University of Manitoba, Winnipeg, Manitoba, R3T 2N2, Canada
Aftab Mufti, Department of Civil Engineering, University of Manitoba, Winnipeg, Manitoba, R3T 2N2, Canada
Douglas Thomson, Department of Electrical and Computer Engineering, University of Manitoba, Winnipeg, Manitoba, R3T 2N2, Canada

INTRODUCTION

Corrosion damage in pre-stressed/post-tensioned concrete beams and girders is an issue of great concern. The steel tendons of concrete bridges can severely corrode over time and lose cross-sectional area between 70% to 100% [1]. A low-cost method of monitoring the progression of corrosion damage in these systems is of great interest. As corrosion damage progresses, wire breaks and bond slipping lead to acoustic emission events. Acoustic emission-based monitoring systems show promising results in monitoring the progression of corrosion damage in steel tendons of pre-stressing/post-tensioning girders [2]–[7]

The literature has mainly focused on detecting a particular type of damage in the tendons, such as stress corrosion cracking or hydrogen embrittlement [3], [8]–[15]. However, the tendons can suffer from general corrosion, pitting corrosion, fretting fatigue and corrosion fatigue [16]. Corrosion can induce wire breaks and/or loss of bond between tendons and concrete/grout and consequently decrease the structure's load-carrying capacity [7], [17]–[19]. Therefore, instead of monitoring the cause of damages or detecting the breaks of wires that make up tendons, tracking the progression of damage can be more practical in evaluating the overall safety of bridges.

Yuyama et al. [20] and Käding et al. [21] conducted experimental investigations on applying acoustic emission to detect tendon breaks in pre-stressed concrete bridges. Yuyama et al. [20] used accelerated corrosion experiments to produce wire breaks, while Käding et al. [21] made the breaks by cutting wires. Breaking or releasing pre-stressed or post-tensioned tendons covered by grout or concrete may fracture grout or concrete and release acoustic emissions [22]. However, Yuyama et al. [20] and Käding et al. [21] did not differentiate between acoustic emission resulting from wire breaks, slipping of the tendon, grout cracking or concrete cracks. Therefore, identifying the cause of acoustic emission is important for developing reliable methods, with minimal false alarms, to monitor damage progression. In this work, acoustic emission from accelerated corrosion in pre-stressed beams yielded was largely attributed to tendon slippage.

In this paper, we conducted accelerated corrosion experiments on a pre-stressed beam with three tendons to study acoustic emission signals released from the beam. The accelerated corrosion experiment was continued over a period of several months until at least one wire from each tendon corroded entirely through. Eight acoustic sensors attached to the beam were used to detect and record acoustic signals during the experiments. At the termination of the experiments, to correlate corrosion and tendon slippage with acoustic emission signals, the beam was sliced into 62 slices each 5 cm thick.

MATERIALS & METHODS

The Experimental Set-up

A 3.15 m long pre-stressed concrete beam with 40 cm width and 27 cm depth was used in this section for the accelerated corrosion experiment (Figure 1). As shown in the figures, the beam had three pre-stressing tendons. To record the AEs, present in the beam, eight sensors with DAQs were installed on the beam using epoxy adhesive

(Gorilla five-minute epoxy). The location of the sensors is shown in Figure 1. The experiment was done in two phases. In the first phase, an opening around the tendon was created by carefully removing the concrete cover over the tendon using a hammer drill and chisel. Then, a water-tight plastic tank (with a hole the same size as the pit in its bottom) glued putty on top of the pit using plumbing epoxy. The details of the experiment and the mounting of the corrosion tank are shown in Figure 2. A stainless steel sheet was used as the cathode, the tendon acted as the anode, and 5% NaCl solution was used as the electrolyte. In the experiments, the corrosion current was 4 mA, and the approximate exposed area of tendons was 120 mm2.

The DAQs sampled AE signals at 920 ksamples/s until a threshold was exceeded. Once this threshold was exceeded, the AE signal was sampled for 77,000 samples at 920 ksamples/s and then the sampled data set was stored on an SD card. To set the threshold for each DAQ, the ball impact calibration method was used [23]. A steel ball bearing with a 7 mm diameter was used in the calibration. The ball was dropped from 25 cm height above the sensor and a distance of 10 cm to the sensor. Thresholds were set so that environmental signals would not trigger saving of a sampled data set but would trigger saving a sampled data set when a ball was dropped. This phase of the accelerated corrosion experiment continued for around five months, and the AE signals collected on the SD card were moved to a laptop once a week. The ball drops were carried out weekly to ensure the ongoing integrity of sensors and DAQs. The DAQ circuit had 100 gain, so the recorded signals were post-processed using MATLAB to compensate for the gain. Figure 3 shows the progress of corrosion in the tendon.

In the second phase, the corrosion tank of the previous phase was removed, and two pits surrounding the remaining two tendons were created. As in the first phase, corrosion

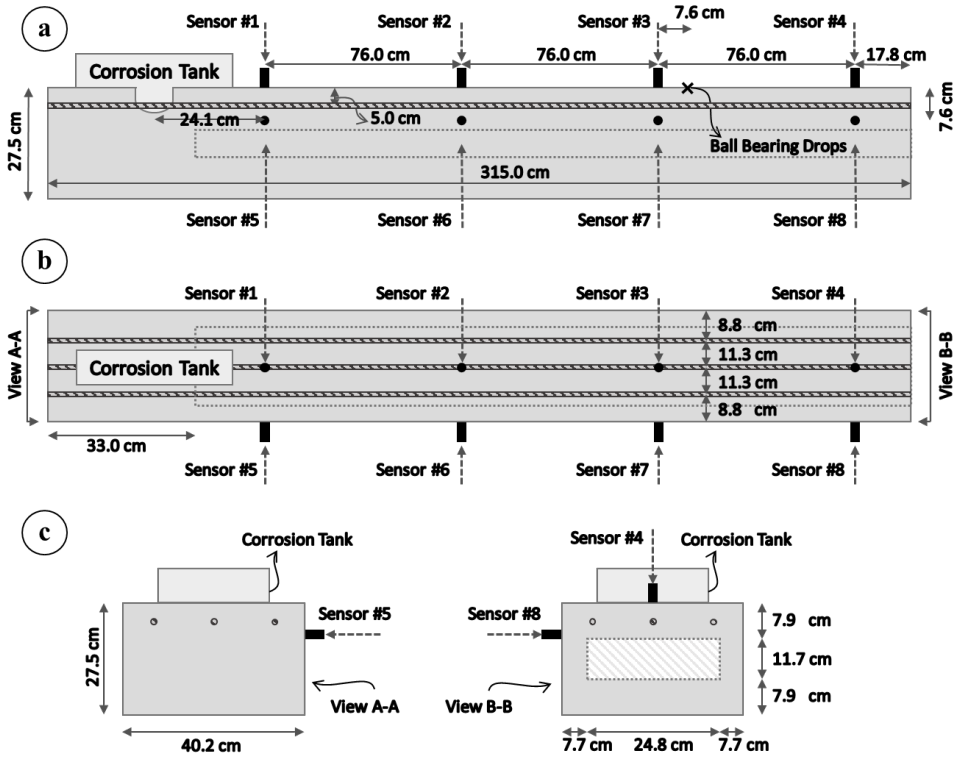

Figure 1. The schematic of the pre-stressed beam and the acceleration corrosion set-up; a) Side view, b) top view, and c) Ends of the beam's view.

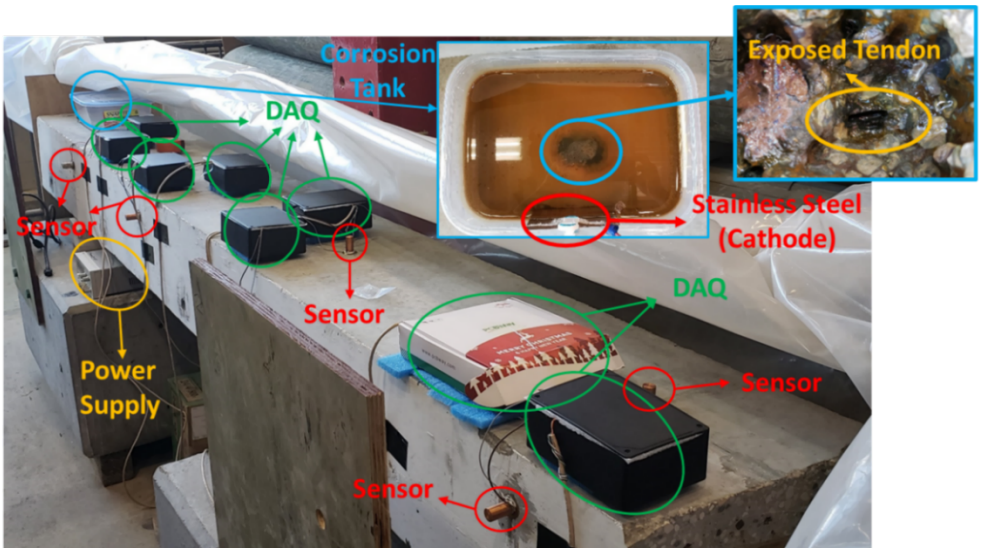

Figure 2. The acceleration corrosion set-up and a corrosion tank.

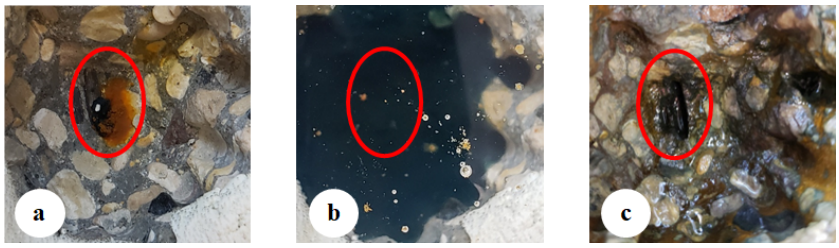

Figure 3. The progress of corrosion over a) 5 days, b) 7 days, and c) 49 days

tanks were installed on the tendons. This phase continued as the first stage and also ended after around five months. Each phase ended when no significant signals were recorded in the preceding month of the experiment.

Localizing Acoustic Signals

As the acoustic signals travel through the medium, they are attenuated. We used attenuation between the sensors to localize the source of recorded acoustic signals. For this purpose, knowing the distance between the sensors, we first estimated the attenuation between the sensors using the ball drop signals. The calculated attenuation was 6.9 dB/m. Then, using the following equation, we localized the sources of recorded events.

$$6.9 = \frac{10}{distance} \log\left(\frac{Power_{sensor\ i}}{Power_{sensor\ j}}\right) \quad (1)$$

Here, the calculated powers of signals for two sensors were used. In some cases, the DAQ measurements were saturated due to large signal magnitude. In these cases, the signals were only analyzed after the time point when none of the DAQ measurements were saturated. Only the portion of the signal after this maximum saturation time were used to calculate signal power. Figure 4 shows an example of an event with saturated signals. Signals of sensors 1 and 2 (Figures 4(a)-(b)) were saturated, the maximum

saturation time among the signals of this event was calculated, then the portion of the signal after this time for all the sensors was used in the calculations.

Visual Inspection of Tendons After Accelerated Corrosion

To visually investigate the condition of the tendons after accelerated corrosion experiments, we have sliced the beam into 62 slices approximately 5cm thick. The cutting process started from the beam's right side (far from the corrosion tanks; see Figure 2). Thus, the tendons' cross sections were visible on each piece's right and left sides.

RESULTS & DISCUSSION

An example of recorded events from the first phase of the experiments is shown in Figure 4. The same trends in signals were observed in sensors 1 to 4 and 5 to 8. Therefore, only signals of sensors 1 to 4 were shown in Figure 4. As seen, signals sensed by sensors 1 and 2 (Figures 4(a)-(b)) were saturated, while the signals of sensors 3 and 4 (Figures 4(c)-(d)) were not. Therefore, the source of this event is expected to be between sensor 2 and the left end of the beam. Using the signal analysis method of Equation 1, the event was estimated to originate between sensors 1 and 2, with a 28 cm distance to sensor 1. Using this same approach, all the AE events were mapped and binned using 31 cm wide bins (Figure 5). The location of the most events can be clustered in three areas; first, between the left end of the beam and corrosion pits; second, between the corrosion pits and 20 cm left of sensor 2; third, between sensor 3 and the right end of the beam. Since no wire breaks were found, these are believed to be due to loss of bond between concrete and tendons near the end of the beam. As the second phase of the accelerated corrosion experiments was done on tendons 1 and 3 simultaneously, therefore, the events were mapped in Figure 5 for both tendons simultaneously.

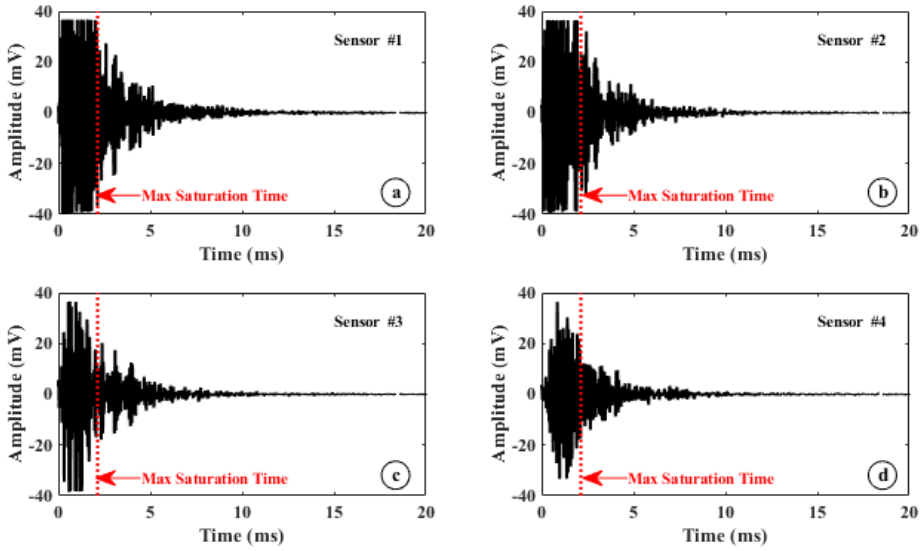

Figure 4. A sample of recorded signals, including both saturated and unsaturated signals from the first phase of experiments.

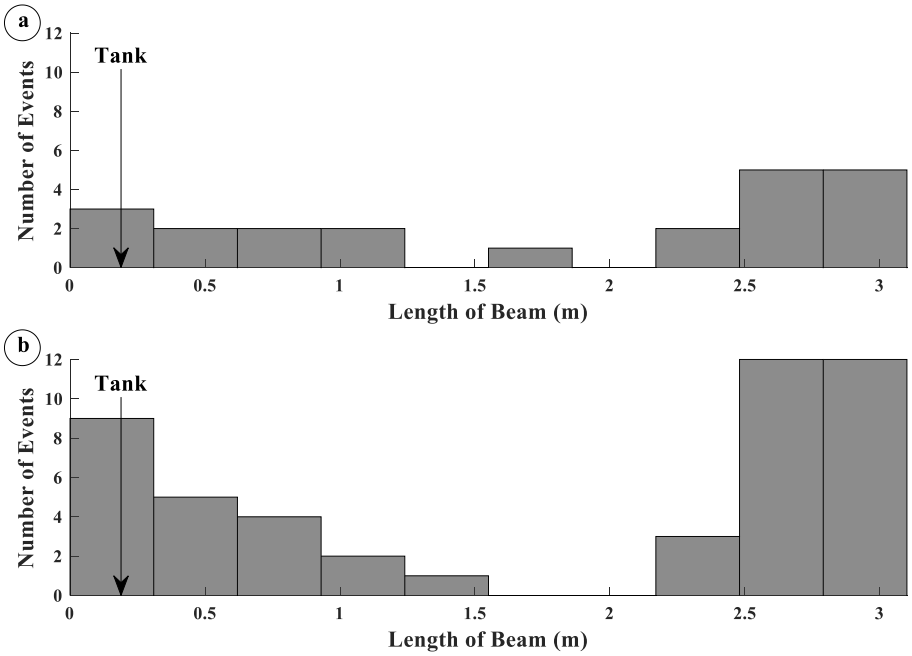

Figure 5. The localized sources of recorded events and the number of their occurrence.

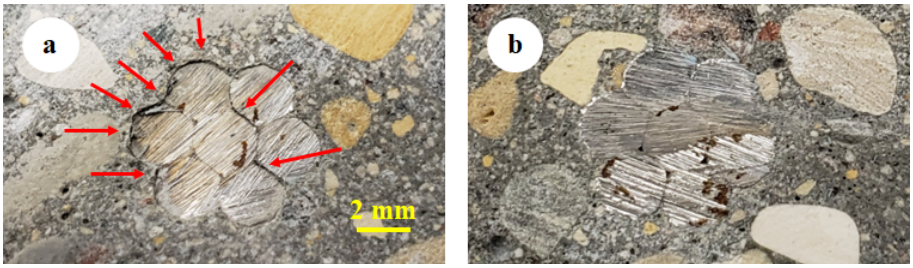

Figure 6. Visual signs of a) losing the bond on the left side and b) keeping the bond on the right side between concrete and tendon 1 of the 25th slice.

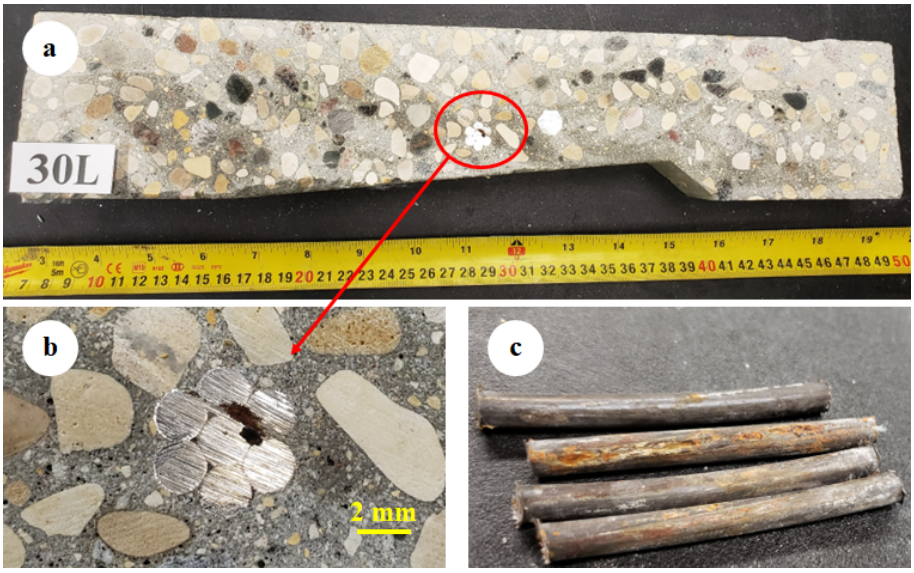

Figure 7. The right side of the 30th slice (a), Visual signs of corrosion on the cross-section of tendon 1 on the left side of the 30th slice (b), and corroded wires of tendon 1 from the 30th slice (c).

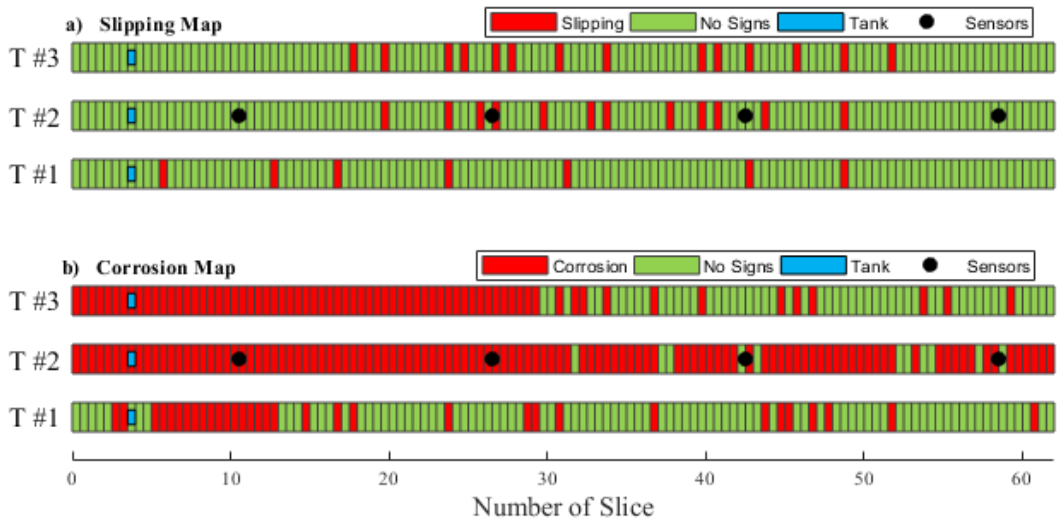

Figure 8. Locations with visible a) slipping and b) corrosion.

Figures 6 and 7 show two typical examples of slice cross-sections. Figure 6 shows tendon 1 on both sides of the 25th slice. As seen, there are signs of losing the bond between the tendon and concrete on the left side. The cutting process was done from right to left, and we have not seen similar signs on the right side of slice 24. Thus we only considered this loss for the left side of tendon 1 in the 25th slice. It should be noted that the slices were numbered from left to right. Figure 7 shows the left side of the 30th slice as well as the visual signs of corrosion on the cross-section of tendon 1 on the left side of the 30th slice. We removed the concrete covering the tendon in this slice and found corroded parts on four wires. Corrosion was more significant on the central wire. The locations of corrosion and slipping tendons were mapped in Figure 8. Corrosion was widespread along tendon 2, with higher concentrations near the corrosion tanks for the other two tendons. There was no obvious correlation with regions of corrosion or loss of bond.

CONCLUSION

In this paper, we used accelerated corrosion experiments to investigate different sources that release acoustic waves when pre-stressing tendons buried in concrete corrode. Acoustic sensors and DAQs were used to detect and record released acoustic waves. The beam was cut into 62 slices in order to inspect the condition of the tendons. The condition of the tendon was obviously not correlated with the origin of the AE signals. The AE signals mechanism is likely the loss of bond between concrete and tendons as wire breaks were not observed. The cumulative number of events within a region is a potential indicator of damage progression. Future work correlating AE event density with loss of structural capacity would be a useful line of study.

REFERENCES

1. Pape, T. M., and R. E. Melchers. 2011. "The effects of corrosion on 45-year-old pre-stressed concrete bridge beams," *Struct. Infrastruct. Eng.*, 7(1–2):101–108.
2. Zaki, A., H. K. Chai, D. G. Aggelis, and N. Alver. 2015. "Non-destructive evaluation for corrosion monitoring in concrete: A review and capability of acoustic emission technique," *Sensors*, 15(8):19069–19101.
3. Appalla, A., M. K. ElBatanouny, W. Velez, and P. Ziehl. 2016. "Assessing Corrosion Damage in Posttensioned Concrete Structures Using Acoustic Emission," *J. Mater. Civ. Eng.*, 28(2) 4015128.
4. Behnia, A., H. K. Chai, and T. Shiotani. 2014. "Advanced structural health monitoring of concrete structures with the aid of acoustic emission," *Constr. Build. Mater.*, 65:282–302.
5. Bayane, I., and E. Brühwiler. 2020. "Structural condition assessment of reinforced-concrete bridges based on acoustic emission and strain measurements," *J. Civ. Struct. Heal. Monit.*, 10(5):1037–1055.
6. Vidya Sagar, R. and B. K. Raghu Prasad. 2013. "Laboratory investigations on cracking in reinforced concrete beams using on-line acoustic emission monitoring technique," *J. Civ. Struct. Heal. Monit.*, 3(3):169–186.
7. Verstrynge, E., C. Van Steen, E. Vandecruys, and M. Wevers. 2022. "Steel corrosion damage monitoring in reinforced concrete structures with the acoustic emission technique: A review," *Constr. Build. Mater.*, 349:128732.
8. Calabrese, L. , G. Campanella, and E. Proverbio. 2013. "Identification of corrosion mechanisms by univariate and multivariate statistical analysis during long term acoustic emission monitoring on a pre-stressed concrete beam," *Corros. Sci.*, 73:161–171.
9. Ramadan, S., L. Gaillet, C. Tessier, and H. Idrissi. 2008. "Detection of stress corrosion cracking of high-strength steel used in prestressed concrete structures by acoustic emission technique," *Appl. Surf. Sci.*, 254(8):2255–2261.
10. Kovač, J., M. Leban, and A. Legat. 2007. "Detection of SCC on prestressing steel wire by the simultaneous use of electrochemical noise and acoustic emission measurements," *Electrochim. Acta*, 52(27):7607–7616.
11. Kovač, J., A. Legat, B. Zajec, T. Kosec, and E. Govekar. 2015. "Detection and characterization of stainless steel SCC by the analysis of crack related acoustic emission," *Ultrasonics*, 62:312–322.
12. Djeddi, L., R. Khelif, S. Benmedakhene, and J. Favergeon. 2013. "Reliability of acoustic emission as a technique to detect corrosion and stress corrosion cracking on prestressing steel strands," *Int. J. Electrochem. Sci*, 8(6):8356–8370.
13. Vélez, W., F. Matta, and P. Ziehl. 2014. "Acoustic Emission Intensity Analysis of Corrosion in Prestressed Concrete Piles," *AIP Conference Proceedings*, 1581(1):888-894.
14. Vélez, W., F. Matta, and P. Ziehl. 2015. "Acoustic emission monitoring of early corrosion in prestressed concrete piles," *Struct. Control Heal. Monit.*, 22(5):873–887.
15. Mangual, J., M. ElBatanouny, P. Ziehl, and F. Matta. 2013. "Corrosion Damage Quantification of Prestressing Strands Using Acoustic Emission," *J. Mater. Civ. Eng.*, 25(9):1326–1334.
16. ACI Committee 222. 2014. "ACI PRC-222.2-14 Report on Corrosion of Prestressing Steels," Farmington Hills, MI, USA.
17. Huo, L., H. Cheng, Q. Kong, and X. Chen. 2019. "Bond-Slip Monitoring of Concrete Structures Using Smart Sensors—A Review," *Sensors*, 19(5):1231.
18. Ho, S. C. M., Ren, L., Labib, E., Kapadia, A., Mo, Y.-L., Li, H., & Song, G. 2015. "Inference of bond slip in prestressed tendons in concrete bridge girders," *Struct. Control Heal. Monit.*, 22,(2):289–300.
19. ElBatanouny, M. K., J. Mangual, P. H. Ziehl, and F. Matta. 2014. "Early corrosion detection in prestressed concrete girders using acoustic emission," *J. Mater. Civ. Eng.*, 26(3):504–511.
20. Yuyama, S., K. Yokoyama, K. Niitani, M. Ohtsu, and T. Uomoto. 2007. "Detection and evaluation of failures in high-strength tendon of prestressed concrete bridges by acoustic emission," *Constr. Build. Mater.*, 21(3):491–500.
21. Käding, M., G. Schacht, and S. Marx. 2022. "Acoustic Emission analysis of a comprehensive database of wire breaks in prestressed concrete girders," *Eng. Struct.*, 270:114846.
22. Shiotani, T., Y. Oshima, M. Goto, and S. Momoki. 2013. "Temporal and spatial evaluation of grout failure process with PC cable breakage by means of acoustic emission," *Constr. Build. Mater.*, 48:1286–1292.
23. McLaskey, G. C., and S. D. Glaser. 2012. "Acoustic Emission Sensor Calibration for Absolute Source Measurements," J. Nondestruct. Eval., 31(2):157–168.